Soft-Magnetic Properties of Nanocrystalline bcc Fe-(Nb, Zr)-B Bulk Alloys Consolidated by Warm Extrusion

Materials Transactions, JIM, Vol. 36, No. 7 (1995), pp. 945 to 951

Soft-Magnetic Properties of Nanocrystalline bcc Fe-(Nb, Zr)-B Bulk Alloys Consolidated by Warm Extrusion

Akinori Kojima*†, Hidehiko Horikiri*††, Akihiro Makino**, Yoshihito Kawamura*, Akihisa Inoue* and Tsuyoshi Masumoto*

*Institute for Materials Research, Tohoku University, Sendai 980-77, Japan
**Central Research Laboratory, Alps Electric Co., Ltd., Nagaoka 940, Japan

We obtained $Fe_{84}Nb_7B_9$ bulk alloys by extruding amorphous powders at temperatures (T_e) between 653 and 723 K and pressures (P_e) of 820 to 1210 MPa, and $Fe_{90}Zr_7B_3$ bulk alloys by extruding at T_e of 673 to 698 K and P_e of 920 to 940 MPa. Subsequent annealing of these bulk alloys at 923 K for 3.6 ks causes the formation of a nanocrystalline bcc phase with grain sizes of 9 to 11 nm for $Fe_{84}Nb_7B_9$ and 20 to 30 nm for $Fe_{90}Zr_7B_3$. The bcc $Fe_{84}Nb_7B_9$ bulk alloy exhibits a magnetization (B_{800}) of 1.40 T, a permeability (μ_e) of 1120 at 300 Hz, and a coercive force (H_c) of 48 A/m in the extrusion condition of T_e=698 K and P_e=870 MPa. Similarly, the B_{800}, μ_e and H_c of the bcc $Fe_{90}Zr_7B_3$ bulk alloy prepared at T_e=698 K and P_e=923 MPa are 1.57 T, 1880 and 29 A/m, respectively. The soft-magnetic properties of the bcc $Fe_{90}Zr_7B_3$ bulk alloy are superior to those of the bcc $Fe_{84}Nb_7B_9$ bulk alloy, presumably because of the formation of a more homogeneous bcc structure for the former alloy.

(Received January 25, 1995)

Keywords: *iron-niobium-zirconium-boron alloy, nanocrystalline bcc structure, high saturation magnetization, soft-magnetic properties, warm extrusion, consolidation*

I. Introduction

Recent miniaturization of electric-magnetic devices has strongly required the fabrication of magnetic materials with higher qualities. New soft-magnetic materials for magnetic heads and transformers must have higher saturation magnetization (B_s) and higher permeability. A large number of studies have been carried out with the aim of developing such new materials.

Recently, Yosizawa *et al.*[1] have reported that good soft-magnetic properties combined with a B_s of 1.3 T are obtained for a mostly single bcc phase with a grain size of about 10 nm prepared by crystallization of the amorphous $Fe_{71.5}Cu_1Nb_3Si_{13.5}B_9$ alloy. The good soft-magnetic properties for the nanocrystalline bcc alloy have been explained on the basis of the magnetization ripple theory[2] and the random anisotropy[3].

More recently, Suzuki *et al.* have carried out[4]-[10] systematic studies on the crystallized structure and magnetic properties of Fe-M-B (M=transition metals) amorphous alloys produced by the melt spinning method and found that a mostly single bcc phase with nanoscale grain size forms as an intermediate crystallized phase of amorphous Fe-M-B (M=Zr, Hf, or Nb) and Fe-M-B-Cu (M=Ti, Zr, Hf, Nb, or Ta) alloy. Subsequently, the nanocrystalline bcc alloys have been found to exhibit significantly low core losses[11] as well as good soft-magnetic properties with a high B_s of 1.7 T, which is higher than that of the nanocrystalline Fe-Cu-Nb-Si-B alloy. Similarly, nanocrystalline bcc Fe-(Zr, Nb)-B thin films prepared by crystallizing the sputtered amorphous phase have been reported to exhibit good soft-magnetic properties with a high B_s of 1.64 T[12][13]. These nanocrystalline bcc Fe-(Zr ,Hf, Nb)-B alloys have been investigated with the aim of using as various types of transformers and magnetic heads. However, the shape of the resulting nanocrystalline alloys is limited to sheet and thin film forms and hence the preparation of bulky nanocrystalline bcc alloys has strongly been demanded for further extension of application fields of the new materials.

In general, amorphous alloys have good engineering properties and have been used in some application fields. However, the shape of amorphous alloys is usually limited to sheet, wire, thin film, and powder and the limitation prevents the extension of its application fields. Consequently, a number of studies on the consolidation of amorphous powders by various methods of explosive compaction[14], high static-pressure compaction[15], and warm extrusion method[16][17] have been carried out for the preparation of bulk amorphous alloys which enable the elimination of the limitation.

The nanocrystalline bcc alloys have higher thermal stability of structure as compared with that of amorphous alloy. It is therefore expected that the nanocrystalline bulk alloy with high B_s and good soft-magnetic properties can be obtained by consolidation of amorphous powders and subsequent annealing of the resultant consolidated alloy.

This paper aims to report the microstructure and magnetic properties of bcc Fe-(Nb, Zr)-B bulk alloys consolidated by a warm extrusion and subsequently annealed.

† On leave from Alps Electric Co., Ltd., Nagaoka 940, Japan.
†† Present address: Gifu Factory, Teikoku Piston Ring Co., Ltd., Kani 509-02, Japan.

II. Experimental Method

Ternary alloys with composition of $Fe_{84}Nb_7B_9$ and $Fe_{90}Zr_7B_3$ were chosen in the present study because they exhibit high permeability and B_s in Fe–(Nb, Zr)–B ternary systems[10]. Alloy ingots were prepared by an arc melting method in an argon atmosphere. Rapidly solidified ribbons with 13 mm in width and 20–30 μm in thickness were produced by a single-roller melt spinning method. Subsequently, the ribbons were ground to powders by using a rotor-speed mill in air at liquid nitrogen temperature, and the powders were ground to the particle size between 53 and 150 μm in an argon atmosphere by using a planetary ball milling machine. We confirmed by X-ray diffractometry that the resulting powders kept an amorphous phase. The powders were packed into a cylindrical container (billet) made of SS41 (JIS) with an outer diameter of 23 mm and an inner diameter of 20 mm as shown in Fig. 1. A core made of either S45C or SKD61 (JIS) was attached along the center of the container with the aim of obtaining a homogeneously consolidated bulk alloy[16]. The billet was evacuated up to less than 1.3×10^{-2} Pa and degassed at 623 K for 900 s. After heating to the extrusion temperatures (T_e) between 653 and 723 K, the billet was extruded at a ram-speed of 2.5 and 5 mm/s through a die with an incidence angle of 90° and a cross-sectional reduction of 40%.

The consolidated bulk alloys were annealed for 3.6 ks at various temperatures ranging from 673 to 1023 K in an evacuated state. Consolidated state of the bulk alloy was examined from optical micrograph of a cross-sectional structure. Density was measured by Archimedian method using toluene or tetrabromoethane, and structure was examined by X-ray diffractometry using Cu-Kα radiation, differential scanning calorimetry (DSC) and thermal mechanical analysis (TMA). Magnetization (B_{800}) was measured by using a vibrating sample magnetometer (VSM) in an applied field of 800 kA/m. Coercive force (H_c) was measured by the use of a dc *B-H* loop tracer in a field of 800 A/m. Effective permeability (μ_e) was measured at 300 Hz under a field of 0.8 A/m for a ring-shaped sample with an inner diameter of 11 mm and an outer diameter of 13 mm. Magnetostriction (λ_s) of ribbon samples was measured by a three probe capacitance method in a field of 240 kA/m. All measurements of the magnetic properties were made at room temperature.

III. Results and Discussion

1. $Fe_{84}Nb_7B_9$ bulk alloys

(1) Production and soft magnetic properties of bulk $Fe_{84}Nb_7B_9$ alloys

The difference between nominal and chemically analyzed compositions for the $Fe_{84}Nb_7B_9$ alloy was less than 1.0 mass% for Nb and 0.2 mass% for B and the impurities mixed from grinder were less than 0.3 mass% for Cr and less than 0.2 mass% for Ni. Therefore, the compositions denoted by subscripts represent the mixing ration of the unalloyed pure elements.

Figure 2 shows the DSC and TMA curves of the melt-spun $Fe_{84}Nb_7B_9$ ribbon heated at a scanning rate of 0.17 K/s. In the DSC curve, an exothermic peak due to the transition of amorphous to bcc phase[10] is seen at about 750 K. The TMA curve indicates that the sample is deformed at a nearly constant rate in the temperature range below about 720 K, and at significantly enhanced rates in the higher temperature range from 720 to 790 K. This change in the deformation rate is due to the softening in the vicinity of the crystallization temperature. By utilizing the softening phenomenon, the consolidation of the amorphous powders was tried.

Figure 3 shows the relation between the extrusion temperature (T_e) and the representative extrusion pressure (P_e) for the amorphous $Fe_{84}Nb_7B_9$ powder extruded in

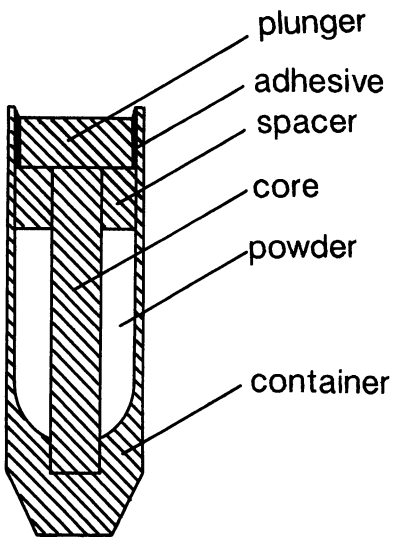

Fig. 1 Schematic illustration of a billet attached a core of S45C or SKD61 in the center.

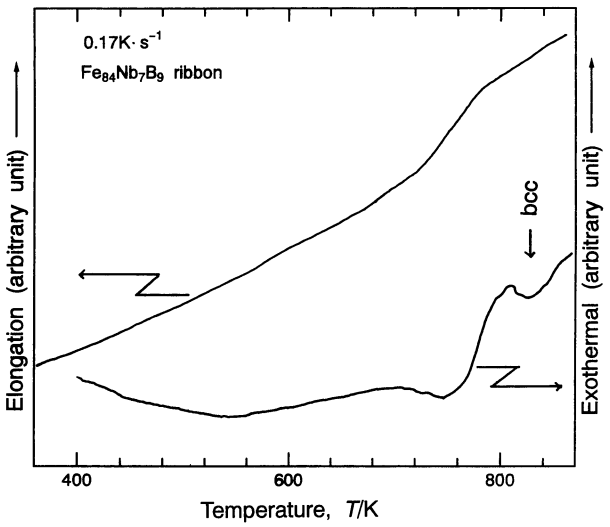

Fig. 2 Differential scanning calorimetric (DSC) and thermal mechanical analytical (TMA) curves of the melt-spun $Fe_{84}Nb_7B_9$ ribbon heated at a scanning rate of 0.17 K/s.

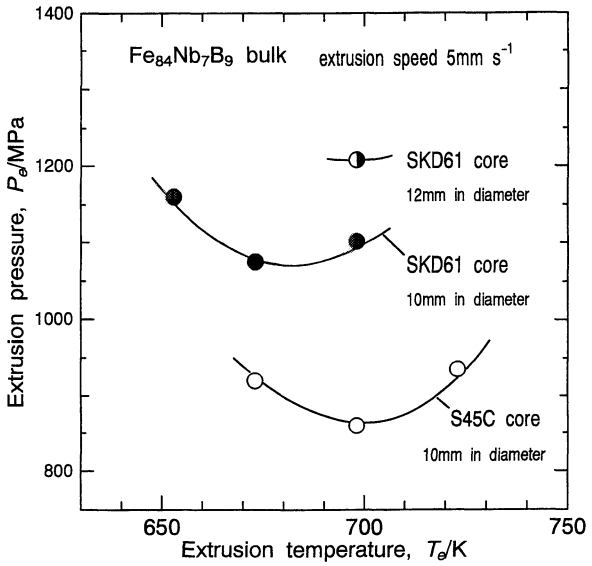

Fig. 3 Relation between the extrusion temperature (T_e) and the representative extrusion pressure (P_e) for the amorphous $Fe_{84}Nb_7B_9$ powder at a ram-speed of 5 mm/s in the use of the billet with S45C or SKD61 core.

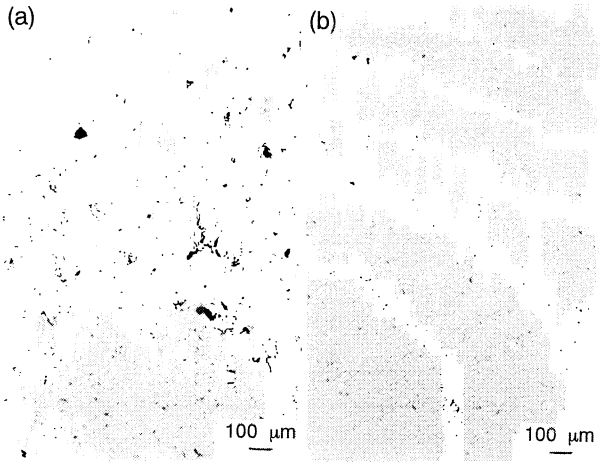

Fig. 4 Optical micrographs of $Fe_{84}Nb_7B_9$ bulk alloys extruded at T_e=673 K and P_e=920 MPa (a), T_e=673 K and P_e=1070 MPa (b).

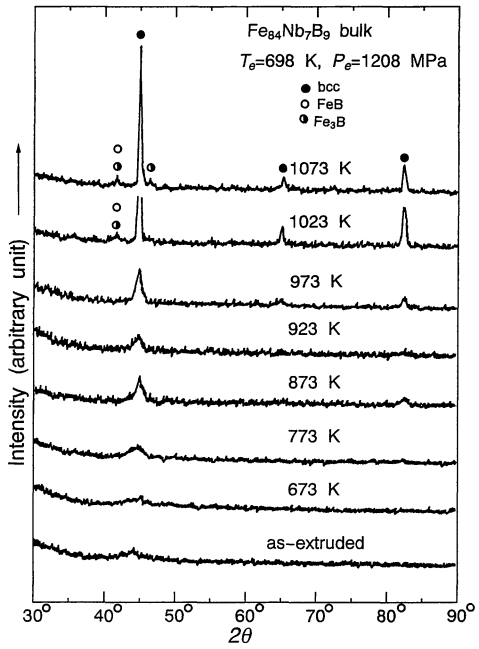

Fig. 5 Change in X-ray diffraction patterns of the $Fe_{84}Nb_7B_9$ bulk alloy extruded T_e=698 K and P_e=1208 MPa in as-extruded state and annealed for 3.6 ks at the temperature (T_a) between 673 and 1073 K.

the use of S45C and SKD61 cores. The value of the P_e shows a minimum at T_e=698 K for the S45C core and 673 K for the SKD61 core, suggesting that the amorphous powder is in the most softening state around these T_e temperatures. One can notice that these temperature are lower than the softening temperature (720–790 K) evaluated from the TMA curve. This difference is due to the deformation-induced heating during the extrusion process. It is seen that the P_e is higher for the SKD61 core than for the S45C core, and also higher for the 12 mm core than for the 10 mm core. This tendency is in agreement with the previous result that extrusion pressure is higher in the case of harder core and bigger core[17], suggesting that we can control P_e by controlling the condition of core.

The optical micrographs of the $Fe_{84}Nb_7B_9$ bulk alloys extruded at T_e of 673 K and P_e of 920 and 1070 MPa are shown in Fig. 4(a) and (b). Some pores are seen in the bulk alloy extruded at P_e=920 MPa, while the bulk at P_e of 1070 MPa is in a rather fully consolidated state. The density of the latter is measured to be about 99% in comparison with the melt-spun ribbon alloy, indicating the necessity of the high extrusion pressure for the achievement of a good consolidated state.

Figure 5 shows the change in the X-ray diffraction patterns for the $Fe_{84}Nb_7B_9$ bulk alloy extruded at T_e of 698 K and P_e of 1208 MPa in as-extruded state and annealed for 3.6 ks at temperatures (T_a) between 673 and 1073 K. A broad halo is seen at a diffraction angle of about 45 degrees for the as-extruded bulk and the annealed bulk at 673 K, suggesting that these bulk alloys are mainly composed of an amorphous phase. For the bulk annealed at 773 K, the diffraction peak corresponding to a bcc phase is seen and the intensity increases significantly with increasing T_a from 773 to 1073 K. One can notice that a mostly single bcc phase is formed in the T_a range from 773 to 973 K. These results are the same as those for the melt-spun amorphous alloy.

The changes in B_{800}, μ_e, and H_c as a function of T_a for the $Fe_{84}Nb_7B_9$ bulk alloys are shown in Fig. 6, along with the data of magnetostriction (λ_s) for the melt-spun ribbon with the same composition. The B_{800} of the as-extruded bulk is in the low range of 0.5 to 0.7 T and increases to about 1.5 T by annealing at T_a above 923 K, accompanying the precipitation of the bcc phase from the amorphous phase. Magnetostriction of the ribbon alloy decreases with increasing T_a and becomes nearly zero in the vicinity of 923 K. It is therefore thought that the magnetostriction of the bulk alloy with the same composition

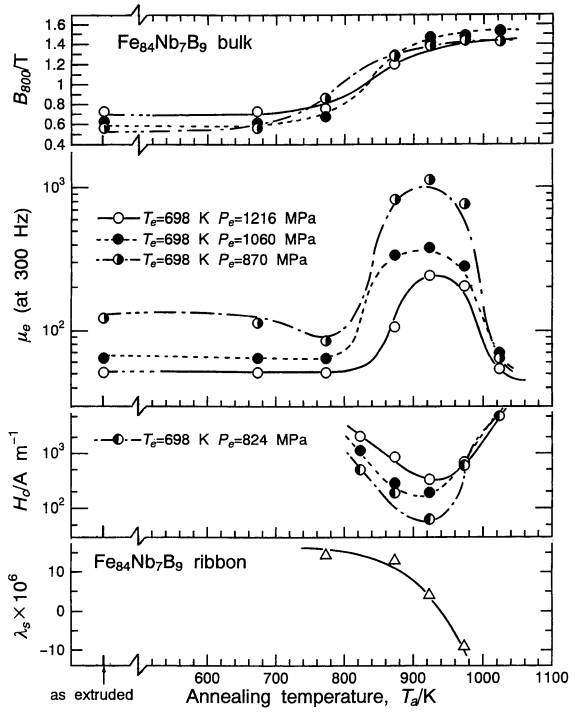

Fig. 6 Changes in the magnetization (B_{800}), effective permeability (μ_e) at 300 Hz and coercive force (H_c) as a function of T_a for the $Fe_{84}Nb_7B_9$ bulk alloys, along with the data of magnetostriction (λ_s) for the melt-spun $Fe_{84}Nb_7B_9$ ribbon.

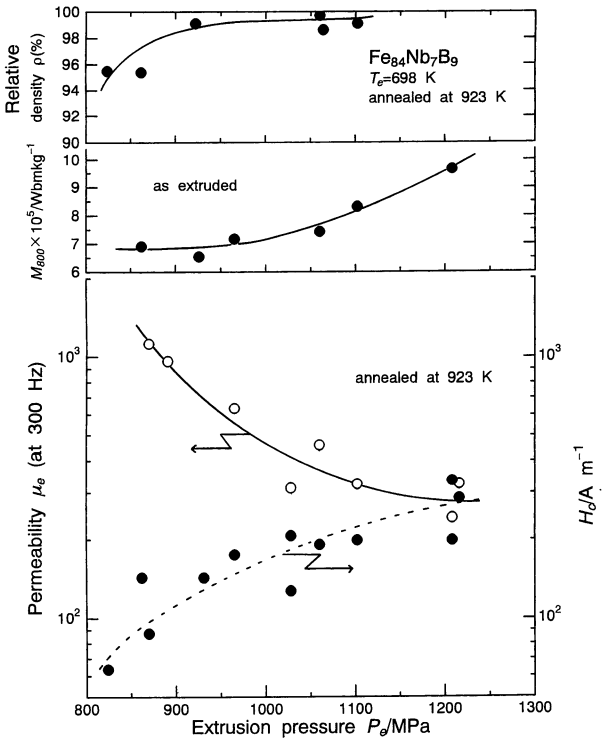

Fig. 7 Dependence of P_e on the relative density (ρ), magnetization ($M_{800}=B_{800}/d$; d=density) and μ_e and H_c for the $Fe_{84}Nb_7B_9$ bulk alloy in as-extruded and annealed (T_a=923 K) states.

is also nearly zero at 923 K because the structure of the bulk alloy is nearly the same as that of the ribbon alloy. Although the μ_e is as low as 200 in the as-extruded state, it increases significantly by annealing at 923 K leading to the phase change from amorphous to bcc phase and the decrease in magnetostriction, accompanying the decrease in H_c. The highest μ_e of 1120 and the lowest H_c of 48 A/m were obtained for the samples extruded at P_e of 824 to 870 MPa. We also investigated the relation between P_e and magnetic properties.

Figure 7 shows the dependence of P_e on the relative density (ρ), magnetization ($M_{800}=B_{800}/d$; d=density), μ_e and H_c for the $Fe_{84}Nb_7B_9$ bulk alloy in as-extruded and annealed (T_a=923 K) states. The high ρ above 99% is obtained for the bulk alloy extruded at P_e above 1000 MPa, but the ρ tends to decrease with decreasing P_e. Besides, the decrease in P_e causes the higher μ_e and the lower H_c in annealed state. These results indicate that it is difficult to obtain a $Fe_{84}Nb_7B_9$ bulk alloy with good soft-magnetic properties and high ρ. The M_{800} of the as-extruded bulk alloy tends to increase with increasing P_e, suggesting that a part of bcc phase has already precipitated in the as-extruded state and the volume fraction of the bcc phase increases for the samples extruded at higher P_e because of the deformation-induced heating.

(2) Microstructure of the $Fe_{84}Nb_7B_9$ bulk alloy

Figure 8 shows the DSC curves at a heating rate of 0.33 K/s for the $Fe_{84}Nb_7B_9$ bulk alloy extruded at T_e=698 K, and P_e=824 and 1216 MPa, along with the

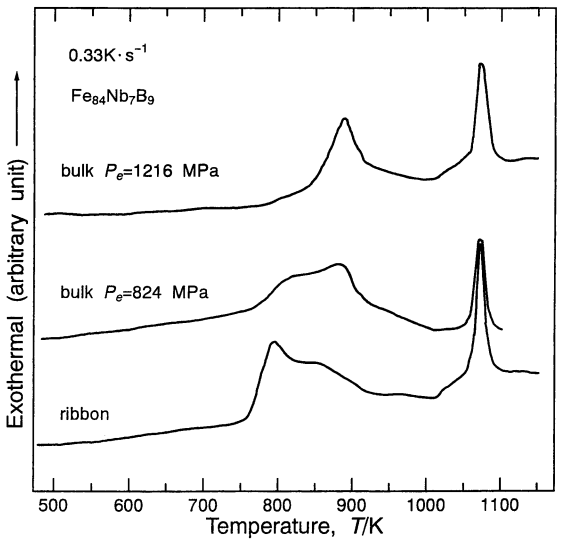

Fig. 8 DSC curves for the $Fe_{84}Nb_7B_9$ bulk alloys extruded at T_e=698 K, and P_e=824 and 1216 MPa, along with the data of the melt-spun ribbon with the same composition.

data of the melt-spun ribbon. It is seen that the first and the second peaks appear between 750 and 950 K, and between 1050 and 1100 K, respectively. The first peak is due to the transition from the amorphous to bcc-Fe phase and the second peak results from the transition from a mostly single bcc phase to mixed phases of bcc-Fe and compounds[10]. The first peak of the bulk alloy is smaller

than that of the ribbon alloy and shifts to the higher temperature side for the sample extruded at higher P_e. These changes indicate that the extruded bulk alloy contains a smaller amount of bcc-Fe phase and the crystalline temperature of the residual amorphous phase increases. This assumption is also supported from the result that the M_{800} in the as-extruded state is higher for the alloy extruded at the higher P_e, as shown in Fig. 7.

Figure 9 shows the changes in the average grain size of bcc-Fe phase (D) for the $Fe_{84}Nb_7B_9$ bulk alloys extruded at T_e=698 K and P_e=824, 1060 and 1208 MPa, along with a bright-field electron micrograph of the bulk alloy extruded at T_e=698 K and P_e=824 MPa. The data of the melt-spun ribbon with the same composition are also shown for comparison. The D value is evaluated from the half width of the X-ray diffraction bcc (110) peak by the use of Scherrer's equation. At T_a=923 K, the D values of the bulk alloys show as small as 9 to 11 nm as similar to that of the ribbon alloy. It is seen that the grain size of the bcc-Fe phase obtained from the TEM images of the bulk alloy is in the range from 10 to 15 nm, which roughly agrees with that obtained from X-ray diffraction. At T_a above 973 K, the D values of the bulk alloys increase with increasing T_a. It is seen the grain growth of the bcc phase occurs more rapidly for the bulk alloy than for the ribbon alloy and for the bulk alloy extruded at higher P_e. Considering that the volume fraction of the bcc phase in the as-extruded state is larger for the bulk alloy extruded at higher P_e, the growth of the pre-existing bcc phase in the as-extruded state is easier as compared with the bcc grain precipitated from amorphous phase by annealing, leading to the formation of an inhomogeneous microcrystalline structure. That is, the inhomogeneity of microcrystalline structure as is evidenced from the large D values is more distinct for the bulk alloy extruded at higher P_e. It is also thought that the inhomogeneous microstructure causes the degradation of soft-magnetic properties for the bulk alloy extruded at higher P_e as shown in Fig. 7.

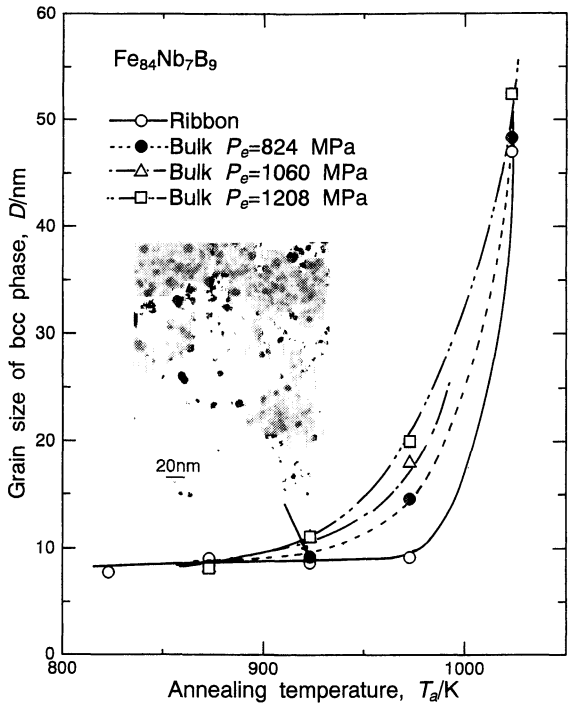

Fig. 9 Changes in the average grain size of bcc-Fe phase (D) for the $Fe_{84}Nb_7B_9$ bulk alloys extruded at T_e=698 K and P_e=824, 1060 and 1208 MPa, and the melt-spun ribbon with the same composition, along with a bright-field electron micrograph of the bulk alloy extruded at T_e=698 K and P_e=824 MPa.

2. $Fe_{90}Zr_7B_3$ bulk alloys

(1) Preparation and soft-magnetic properties of bulk $Fe_{90}Zr_7B_3$ alloys

Figure 10 shows the DSC curve of the melt-spun $Fe_{90}Zr_7B_9$ ribbon at a heating rate of 0.17 K/s, along with that of the $Fe_{84}Nb_7B_9$ ribbon. The crystallization of the $Fe_{90}Zr_7B_3$ alloy occurs at a higher temperature as compared with that for the $Fe_{84}Nb_7B_9$ ribbon alloy.

An optical micrograph of the $Fe_{90}Zr_7B_3$ bulk alloy extruded at T_e=698 K and P_e=923 MPa is shown in Fig. 11. A rather densely consolidated state with high relative density above 99% is obtained for the sample, presuma-

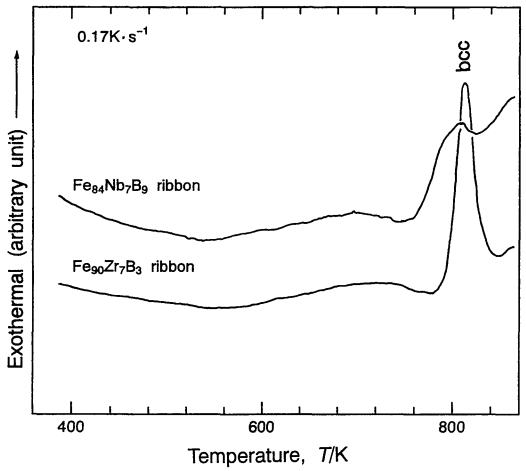

Fig. 10 DSC curves of the melt-spun $Fe_{90}Zr_7B_9$ and $Fe_{84}Nb_7B_9$ ribbons at a heating rate of 0.17 K/s.

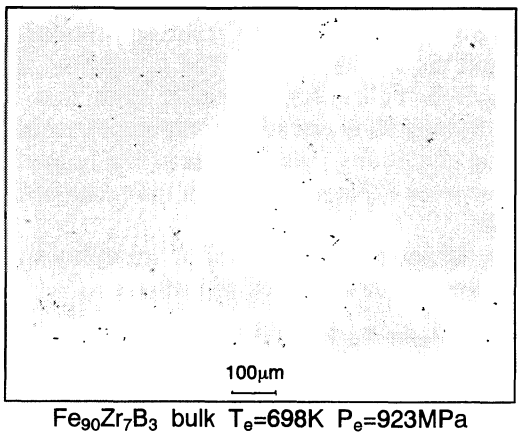

Fig. 11 The optical micrograph of the $Fe_{90}Zr_7B_3$ bulk alloy extruded at T_e=698 K and P_e=923 MPa.

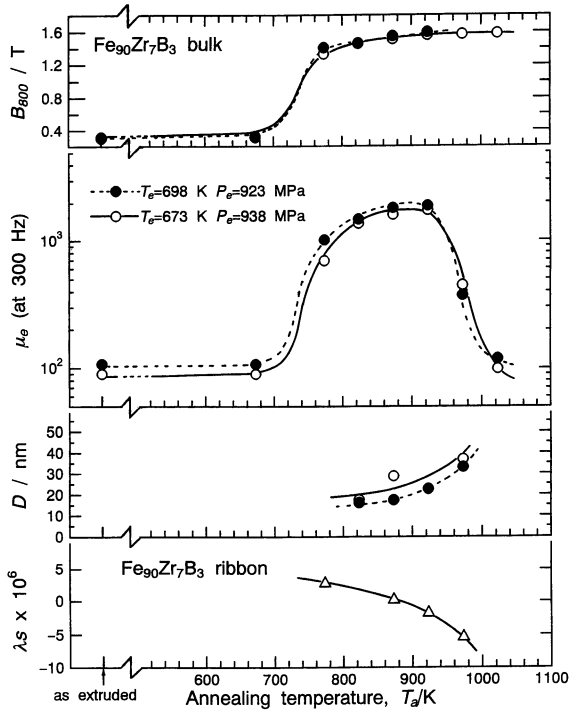

Fig. 12 Changes in B_{800}, μ_e, and average grain size of bcc-Fe phase (D) as a function of T_a for the $Fe_{90}Zr_7B_3$ bulk alloys extruded at T_e=698 K and P_e=923 MPa, and T_e=673 K and P_e=938 MPa, along with the data of magnetostriction (λ_s) of the melt-spun ribbon.

bly because of the relatively high P_e.

Figure 12 shows the changes in B_{800}, μ_e, and average grain size of bcc-Fe phase (D) as a function of T_a for the $Fe_{90}Zr_7B_3$ bulk alloy extruded at T_e=698 K and P_e=923 MPa, and T_e=673 K and P_e=938 MPa along with the magnetostriction (λ_s) of the melt-spun ribbon. The B_{800} in the as-extruded state shows low values of about 0.3 T and increases to about 1.6 T by annealing at T_a above 773 K, accompanied by the transition from the amorphous to bcc phase. The λ_s of the ribbon decreases with increasing T_a and becomes nearly zero in the vicinity of 923 K, indicating that the λ_s of the bulk alloy is nearly zero at 923 K. The μ_e in the as-extruded state is low, but the subsequent annealing at T_a ranging from 773 to 923 K causes the increase in μ_e to a maximum value of 1880, accompanying the transition from amorphous to bcc phase and the decrease of λ_s. The μ_e value of 1880 for the $Fe_{90}Zr_7B_3$ bulk alloys is higher than that for the $Fe_{84}Nb_7B_9$ bulk alloy extruded at the same extrusion and annealing conditions. The D value of the bulk alloy annealed between 823 and 923 K is in the range of from 15 to 30 nm.

When the sample is composed of amorphous and bcc phases, B_{800} can be expressed as follows.

$$B_{800}=B_{bcc}V_b/100+B_{amo}V_a/100 \quad (1)$$

$$V_a+V_b=100 \quad (2)$$

Here, B_{bcc} and B_{amo} are the magnetization values of the bcc and amorphous phases, respectively, and V_b and V_a are the volume fractions (%) of their constituent phases. Equation (3) is derived from eqs. (1) and (2).

$$V_b=(B_{800}-B_{amo})\times 100/(B_{bcc}-B_{amo})(\%) \quad (3)$$

If the density of the bcc phase is assumed to be nearly equal to that of the amorphous phase, eq. (4) is obtained.

$$V_b=(M_{800}-M_{amo})\times 100/(M_{bcc}-M_{amo})(\%) \quad (4)$$

It is assumed that M_{amo} is roughly equal to the M_{800} of the melt-spun ribbon because of the formation of a single amorphous phase and M_{bcc} is roughly equal to the M_{800} of the bulk alloy annealed at T_a=973 K because of the formation of a mostly single bcc phase. The V_b values in the as-extruded state for the $Fe_{84}Nb_7B_9$ bulk alloy extruded at T_e=698 K and P_e=824 MPa, and $Fe_{90}Zr_7B_3$ bulk alloy extruded at T_e=698 K and P_e=923 K are roughly evaluated by substituting M_{800}, M_{amo}, and M_{bcc} into eq. (4).

$$V_{b1}=11\% \quad \text{for} \quad Fe_{84}Nb_7B_9 \quad (5)$$

$$V_{b2}=5\% \quad \text{for} \quad Fe_{90}Zr_7B_3 \quad (6)$$

Thus, the amount of the bcc phase in the as-extruded state is smaller for the $Fe_{90}Zr_7B_3$ bulk than the $Fe_{84}Nb_7B_9$ bulk, suggesting that the nanocrystalline structure formed by annealing is more homogeneous for the former bulk than the latter bulk. The high degree of homogeneity of nanocrystalline structure seems to cause the higher μ_e for the $Fe_{90}Zr_7B_3$ bulk as shown in Fig. 12.

Figure 13 shows the DSC curves for the $Fe_{90}Zr_7B_3$ bulk alloys extruded at T_e=698 K and P_e=923 MPa, and T_e=673 K and P_e=938 MPa with a heating rate of 0.33 K/s, along with the data of the melt-spun ribbon. The two exothermic peaks are seen for all the samples. The first peak with higher intensity is due to the transition from the amorphous to bcc phase and the second peak with lower intensity due to the transition from the bcc phase to mixed phase of bcc and compounds[10]. One can not notice an obvious difference in the first peek between the bulk and the ribbon. The pre-existed bcc phase is small in the as-extruded state and the crystallization tem-

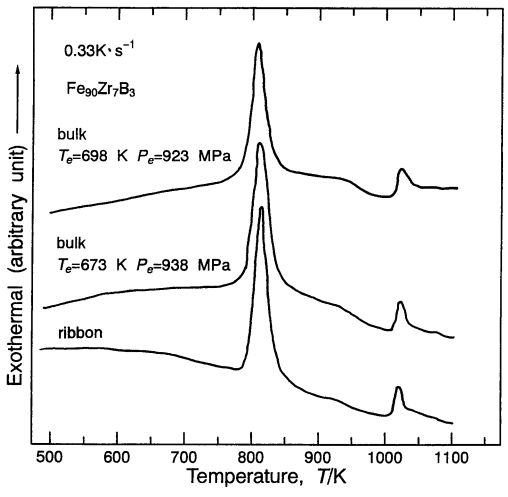

Fig. 13 DSC curves for the $Fe_{90}Zr_7B_3$ bulk alloys extruded at T_e=698 K and P_e=923 MPa, and T_e=673 K and P_e=938 MPa, along with the data of the melt-spun ribbon with the same composition.

Table 1 B_{800}, μ_e and H_c values for the $Fe_{84}Nb_7B_9$ and $Fe_{90}Zr_7B_3$ bulk alloys extruded at T_e=698 K and P_e=870 MPa, and T_e=698 K and P_e=923 MPa, respectively.

Alloy	B_{800}/T	μ_e (at 300 Hz)	H_c/Am^{-1}
$Fe_{84}Nb_7B_9$ bulk T_e=698 K, P_e=870 MPa	1.40	1120	48
$Fe_{90}Zr_7B_3$ bulk T_e=698 K, P_e=923 MPa	1.57	1880	29

perature of the residual amorphous phase is close to that of the amorphous phase in the melt-spun ribbon. This is consistent with the present result that V_{b2} is smaller than V_{b1}.

Table 1 shows the B_{800}, μ_e and H_c values for the $Fe_{84}Nb_7B_9$ and $Fe_{90}Zr_7B_3$ bulk alloys extruded at T_e=698 K and P_e=870 MPa, and T_e=698 K and P_e=923 MPa, respectively. The $Fe_{90}Zr_7B_3$ bulk shows a higher B_{800} of 1.57 T, a higher μ_e of 1880, and a lower H_c of 29 A/m which exceed those for the $Fe_{84}Nb_7B_9$ bulk alloy in addition to the high ρ.

IV. Summary

The consolidation of the amorphous $Fe_{84}Nb_7B_9$ and $Fe_{90}Zr_7B_3$ powders was tried by warm extrusion method and the structure and magnetic properties of the resulting consolidated bulk alloy were examined in as-extruded and annealed state. The results obtained are summarized as follows,

(1) By utilizing the phenomenon that the amorphous powders are soften in the vicinity of crystallization temperature, the bulk alloys were prepared by extrusion at T_e=653 to 723 K and P_e=820 to 1210 MPa for the $Fe_{84}Nb_7B_9$ powders and at T_e=673 to 698 K and P_e=920 to 940 MPa for the $Fe_{90}Zr_7B_3$ powders.

(2) The $Fe_{84}Nb_7B_9$ and $Fe_{90}Zr_7B_3$ bulk alloys were composed of an amorphous phase containing a small amount of the bcc phase in the as-extruded state, and the constituent phase changes to a mostly single bcc phase after annealing. The grain size of the $Fe_{84}Nb_7B_9$ and $Fe_{90}Zr_7B_3$ bulk alloys annealed at 923 K was in the range of 9 to 11 nm and 20 to 30 nm, respectively.

(3) The consolidated state of the $Fe_{84}Nb_7B_9$ bulk alloy was better for the sample extruded at higher P_e and the relative density of the bulk alloy extruded at P_e above 1000 MPa was above 99% in comparison with that of the melt-spun ribbon.

(4) The μ_e and H_c of the $Fe_{84}Nb_7B_9$ bulk alloy annealed at 923 K were higher and lower, respectively, as compared with those for the bulk alloy extruded at higher P_e. The $Fe_{84}Nb_7B_9$ bulk alloy extruded at T_e=698 K and P_e=870 MPa showed a B_{800} of 1.40 T, a μ_e of 1120 at 300 Hz, and a H_c of 48 A/m.

(5) The $Fe_{90}Zr_7B_3$ bulk alloy extruded at T_e=698 K and P_e=923 MPa was in a rather densely consolidated state with the relative density above 99% and exhibited a B_{800} of 1.57 T, a μ_e of 1880 at 300 Hz, and a H_c of 29 A/m. The soft-magnetic properties of the $Fe_{90}Zr_7B_3$ bulk alloy were superior to those of the $Fe_{84}Nb_7B_9$ bulk presumably because the former alloy had the more homogeneous microstructure.

Acknowledgments

The authors wish to thank Mr. K. Hangai of Central laboratory in Alps electric Co., Ltd. for the magnetic measurements.

REFERENCES

(1) Y. Yosizawa, S. Oguma and K. Yamauchi: J. Appl. Phys., **64** (1988), 6044.
(2) H. Hoffman: J. Appl. Phys., **35** (1964), 1790.
(3) G. Herzer: Mater. Sci. Eng., **A113** (1991), 1.
(4) K. Suzuki, N. Kataoka, A. Inoue, A. Makino and T. Masumoto: Mater. Trans., JIM, **31** (1990), 743.
(5) K. Suzuki, A. Makino, N. Kataoka, A. Inoue and T. Masumoto: Mater. Trans., JIM, **32** (1991), 93.
(6) K. Suzuki, M. Kikuchi, A. Makino, A. Inoue and T. Masumoto: Mater. Trans., JIM, **32** (1991), 961.
(7) K. Suzuki, A. Makino, A. Inoue and T. Masumoto: Jpn. J. Appl. Phys., **30** (1991), L1729.
(8) K. Suzuki, A. Makino, A. Inoue and T. Masumoto: J. Appl. Phys., **70** (1991), 6232.
(9) K. Suzuki, A. Makino, A. Inoue and T. Masumoto: J. Japan Inst. Metals, **57** (1993), 964.
(10) K. Suzuki, A. Makino, A. Inoue and T. Masumoto: J. Appl. Phys., **74** (1993), 3316.
(11) A. Makino, K. Suzuki, A. Inoue and T. Masumoto: Mater. Trans., JIM, **32** (1991), 551.
(12) A. Makino, K. Suzuki, A. Inoue and T. Masumoto: Mater. Trans., JIM, **33** (1992), 80.
(13) A. Makino, S. Arano, A. Inoue and T. Masumoto: J. Japan Inst. Metals, **58** (1994), 106.
(14) M. Takagi, Y. Kawamura, M. Araki, Y. Kuroyama and T. Imura: Mater. Sci. Eng., **98** (1988), 457.
(15) Y. Kawamura, M. Takagi, M. Senoo and T. Imura: Mater. Sci. Eng., **98** (1988), 415.
(16) Y. Kawamura, M. Takagi and M. Akai: Mater. Sci. Eng., **98** (1988), 449.
(17) Y. Kawamura, A. Inoue and T. Masumoto: J. Japan Inst. Metals, **57** (1993), 804.